A hybrid drought index for drought assessment in Wadi Shueib catchment area in Jordan

Odai Al Balasmeh, Richa Babbar and Tapas Karmaker

ABSTRACT

Wadi Shueib catchment in Jordan is a water stress area and climate change is creating a further deficiency in precipitation, streamflow, and soil moisture; which are a deterrent to agriculture production in the area. In order to analyze the drought-like situation in the area, a hybrid drought index (HDI) has been developed considering the combined effect of these three variables. Fuzzy analytical hierarchy process (F-AHP) and entropy weight methods were carried out to develop a hybrid drought index (HDI) which combines meteorological, hydrological, and agricultural drought indices based on precipitation, streamflow, and soil moisture data in the area. The wavelet transform (WT) with cross wavelet (XCT) and wavelet coherence (WTC) were applied to investigate the interaction and the relations between the HDI index, drought indices, and large-scale sunspot activity Niño3.4 index. The results show that HDI can easily capture the trend of the drought-like conditions in the area based on the available data. The trend analysis of HDI revealed an increasing trend in the drought incidences in the near future. The study can be used as an early alarm for drought in the area, which can be helpful in the decision-making process towards water resources planning and management in the future.

Key words | drought indices, entropy weight method, fuzzy-AHP, hybrid drought index (HDI), wavelet cross transform

Odai Al Balasmeh (corresponding author)
Richa Babbar
Tapas Karmaker
Department of Civil Engineering,
Thapar Institute of Engineering and Technology,
Patiala 147004,
Punjab
E-mail: *odaibalaking@gmail.com*

HIGHLIGHTS

- The drought indices representing meteorological, hydrological, and agriculture have been computed and the trend analysis performed.
- The hybrid drought index is developed based on fuzzy set theory.
- HDI confirms an increasing trend in the drought, in the area based on the trend analysis.
- Based on wavelet analysis, the drought variation is found to be mainly dominated by the periodicity of 1 year.

doi: 10.2166/hydro.2020.038

GRAPHICAL ABSTRACT

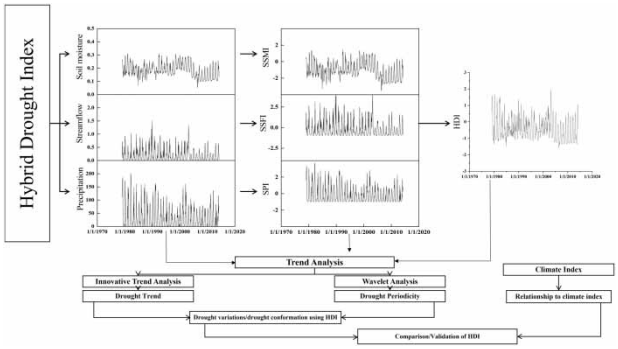

INTRODUCTION

Drought is one of the most critical global issues faced by countries, especially in arid and semi-arid regions. Based on the IPCC report (2014), global climate change in terms of increasing surface temperature is causing an increase in evaporation, resulting in an increase in the incidences of drought and its trend (Griggs & Noguer 2002). Similar to floods, the analysis of drought events (e.g. characteristics and causes) is very important for early warning (Hayes *et al.* 2004). Drought can be classified into four major categories: meteorological drought, agricultural drought, hydrological drought, and socioeconomic drought (Heim 2002). Meteorological drought is related to the deficiency in precipitation over the region and is based on average rainfall with respect to time, while agricultural and hydrological droughts are related to insufficient water, which is required for crop growth and other uses such as water supply, respectively (Wilhite & Glantz 1985). Socioeconomic drought indicates a situation where the water supply becomes insufficient to achieve water demand, thus affecting the society, economy, and environment (Zseleczky & Yosef 2014). Incidence of a drought can be characterized in terms of its duration, severity and spatial distribution (Mishra & Singh 2010; Huang *et al.* 2015; Oertel *et al.* 2018; Yang *et al.* 2020).

Thus, in an attempt to characterize drought, researchers often resort to several approaches and techniques to obtain an insight of drought phenomenon. These approaches can be as simple as using one variable to integrating more than one variable that may have caused drought. Either way, the drought indicator so obtained is a better way of communicating the characteristics of drought in an area (Mishra & Singh 2010; Oertel *et al.* 2018). McKee *et al.* (1993) established a standardized precipitation index (SPI) to determine the severity of drought conditions, based on precipitation time series data. Nury & Hasan (2016) discussed drought conditions based on only SPI and tried to analyze the trend and pattern of rainfall to determine the transient variations in northwestern Bangladesh.

However, a drought is a multivariate phenomenon and its effects exhibit multi-dimensional characteristics. Droughts are found to be influenced by local geography, soil parameters and vegetation, and these factors affect its development and localized severity. Simple indices that depend on one variable to define the drought in an area are usually faced with the difficulty of completely capturing the drought onset and its terminus (Hao & AghaKouchak 2013; Zhu *et al.* 2018). Therefore, it has been found that one-dimensional analysis is inadequate or unreliable to characterize the probabilistic nature of drought occurrence. Recently, several studies have proposed various techniques to combine different drought variables (e.g. precipitation, streamflow, soil moisture, etc.). These studies, however, differ in terms of the methodology chosen to integrate the variables of interest, such that a drought is decomposed to the variable predominantly causing the phenomenon. Each methodology selected also comes with its limitations

in terms of its application and gives a further scope of improvement in the methodology. Kao & Govindaraju (2010) used the copula function to capture the joint behavior of precipitation and streamflow to assess droughts. Hao & AghaKouchak (2013) developed a multivariate standardized drought index (MSDI) combining SPI and the standardized soil moisture index (SSMI) to monitor drought based on copula function. Huang *et al.* (2015) proposed an integrated method using a nonparametric multivariate drought index to combine meteorological and hydrological drought information. Rajsekhar *et al.* (2015) combined meteorological, hydrological and soil moisture to develop a multivariate drought index. Kwon *et al.* (2019) studied the drought characteristics in South Korea by combining the meteorological and agriculture drought using a copula family and grouped the HDI by using the hierarchical agglomerative clustering approach for classifying regional patterns. These studies used a copula probability family to build an integrated drought index. Application of the copula approach has not only been used in assessing drought but also in handling flood extremes. Drought and floods as two weather extremes have often been studied with similar approaches. Numerous studies have used a multivariate concept including the couple approach for flood analysis in the area (e.g. Favre *et al.* 2004; Zhang & Singh 2006; Jongman *et al.* 2014). Atmospheric blocking was found to be one of the most important parameters associated with extreme weather events such as drought and flood, as studied by researchers (Scherrer *et al.* 2006; Sillmann & Croci-Maspoli 2009). Ionita *et al.* (2015) studied flood patterns in Europe based on a combination of different variables such as precipitation, soil moisture, and water lever using multiple linear regression models to predict the streamflow of Elbe River.

The copula probability family has been observed to have certain limitations such as the data is required to follow a probability density function for the usage of this technique and there is a lack of flexibility in the model structure in cases where more than three variables are integrated together (Rajsekhar *et al.* (2015). It has also been observed that there is a possibility of obtaining negative values of the integrated index (Erhardt & Czado 2018). According to Real-Rangel *et al.* (2020), the use of a copula family to build an integrated drought index shows severe deficits, especially when the influencing variables are more than one, then it can only marginally detect a drought-like condition.

Zhu *et al.* (2018) proposed an integrated hybrid drought index based on the entropy weight method with a fuzzy set theory to combine meteorological, hydrological, and agricultural information. Under normal conditions, the entropy method is used to determine the subjective and objective weight while exploiting the entire original data. Now, since it cannot reflect the knowledge of experts and decision-makers, hence it has the disadvantage of causing large fake weights (Roodposhti *et al.* 2016). Zhao *et al.* (2017) proposed the F-AHP method to determine the objective weight, as it has the ability to reflect the knowledge of experts and decision-makers. A fuzzy approach to integrating the variables in an index has several other advantages, namely, the boundaries which separate the index categories are fuzzy (Wilhite & Glantz 1985). Therefore, the variable fuzzy set theory can be applied to characterize vague phenomena and capture their dynamic processes so as to better arrive at a hybrid drought index. Huang *et al.* (2015) and Zhu *et al.* (2018) successfully applied fuzzy set theory to combine meteorological, hydrological, and agricultural factors and proposed an integrated drought index (IDI). However, in these studies the results of IDI were compared only with SPI and the standardized streamflow index (SSFI), regardless of any information about soil moisture or its related drought indicator.

The application of fuzzy set theory to arrive at an index has proved its efficacy in understanding drought phenomenon. In this proposed study, the weights for the aggregating of the three variables will be computed based on the fuzzy-AHP method, which is expected to overcome the limitation of the entropy weight assignment method yet allowing the fuzzy theory to be used for its advantages. Second, we also envisage incorporating three variables in one index, and the index will be validated using trend and wavelet analysis, in contrast to other similar indexes in the literature.

This study attempts to develop a hybrid drought index for Wadi Shueib catchment in Jordan. Jordan is in an arid and semi-arid region of the Middle East and the country is suffering from acute shortages of water with the annual portion per person not exceeding 500 m^3 (Al-Ansari 2016). The future trend of water is declining; thus, this issue is expected

to be deep-seated and serious in the future (Bazzaz 1993). Of all the Middle East countries, Jordan is considered the second poorest country in terms of water in the world. The economy of Jordan mainly depends on agriculture, with limited arable lands in the arid and semi-arid zones.

Different studies have studied the water supply and drought conditions in Jordan. Tarawneh (2011) discussed the water supply in Jordan under drought conditions, and showed that Jordan is under water stress even during rainy seasons (October–May). Törnros & Menzel (2014) addressed the drought based on precipitation, evapotranspiration, and a normalized difference vegetation index (NDVI), and found that drought will increase the irrigation water demand for the agriculture sector in Jordan valley. Recently, Rajsekhar & Gorelick (2017) investigated drought conditions in the Jordan valley under current and future climate change conditions. In their study, precipitation, streamflow, and soil moisture were used. Based on historical data, they concluded that drought conditions will be more severe in the future. Also, Mohammad *et al.* (2018) discussed the impact of natural conditions on drought events in the Yarmuk basin in northern Jordan. The study compared the SPI and standardized water level index (SWI). Gilbert (2017) found that the drought frequency in Jordan is increasing, with almost twice as many winter droughts from 1961 to 2010 as had occurred between 1901 and 1960. Future predictions are that there will be an increase in temperature and decrease in precipitation trends during the winter season (Shakhatreh 2010; Al Balasmeh *et al.* 2019).

The aim of this study is to develop and validate a hybrid drought index for the study area. This aim has been fulfilled through the following objectives:

1. To develop drought indices based on each of the three variables, i.e., precipitation, streamflow, and soil moisture.
2. To compare entropy weight method and fuzzy-AHP method in assigning the weights to the three variables.
3. To perform wavelet analysis to validate the association in time series of each drought index and the hybrid index.
4. To establish the hybrid index by evaluating and comparing the trend analysis of each drought index with the hybrid index.

MATERIAL AND METHODS

Study area

The study site is located in the eastern part of Jordan Valley and west of the salt city (Figure 1). Wadi Shueib is approximately 180 km^2 in size and lies between 31°50′–32°02′ N and 35°35′–35°50′ E. The area has a steep slope with elevation ranging from 200 m below mean sea level (b.m.s.l) at Jordan valley to 1,200 m above mean sea level (a.m.s.l.) near the salt city. Wadi Shueib dam is the outlet of Wadi Shueib catchment, which is used to cater for irrigating the agriculture fields and groundwater recharge purposes in Jordan valley.

Drought analysis

Data collection

In this study, SPI, SSFI, and SSMI were calculated and then further used to compute a hybrid index. Precipitation, streamflow and soil moisture are the main inputs required for the determination of these indices. The precipitation data of 44 years were collected from the Ministry of Water and Irrigation, Jordan, and soil moisture was obtained from the European Space Agency (ESA) Climate Change Initiative soil moisture version 3.3. The available data covered $0.25 \times 0.25°$ resolution daily data from 1978 to present. The soil moisture was found based on average values of square cells in and around the watershed. The data was further divided into two major seasons, rainy (October–May) and summer months (June–September). However, streamflow data for the same time period was not available, and hence the Soil and Water Assessment Tool (SWAT) watershed model was calibrated and verified for predicting the monthly streamflow data for the same time period as the other two variables. SWAT is a physically distributed model used to estimate streamflow, sediment yield, and water quality in agricultural areas based on the interaction of land management practices with climate variables and soil cover (Arnold *et al.* 1998).The following water balance equation is used to measure the hydrologic

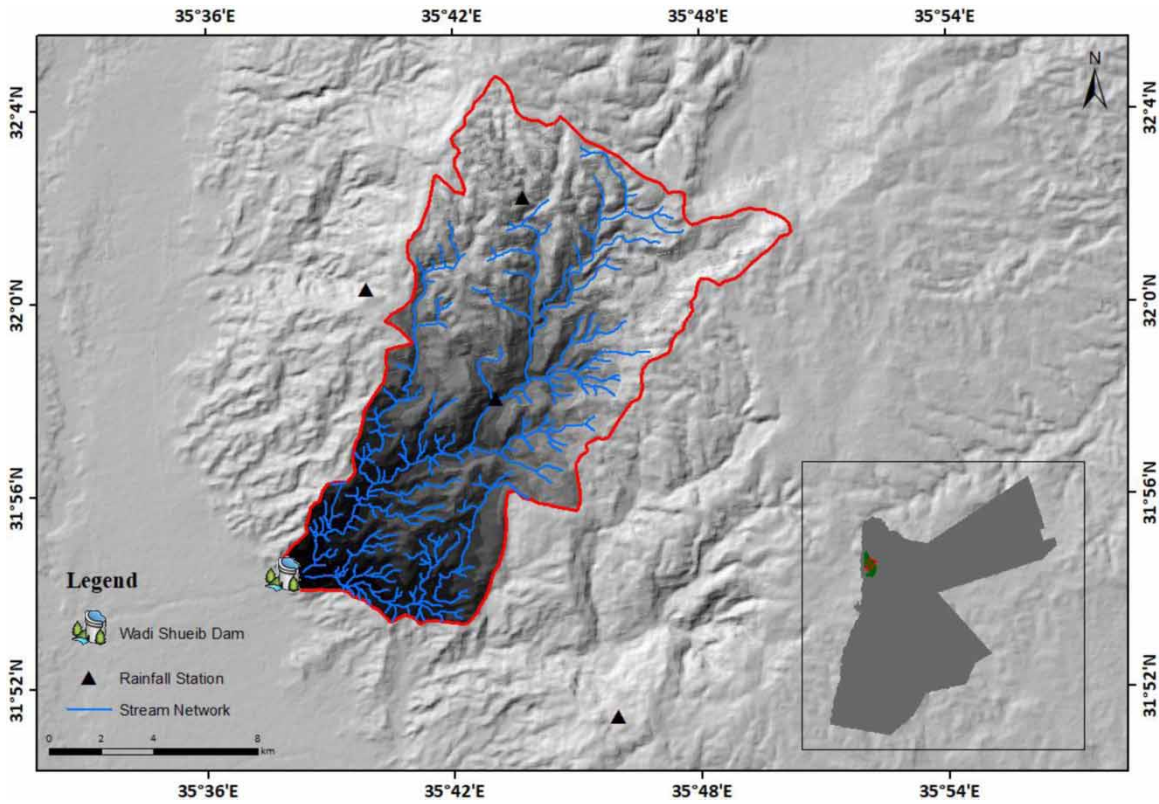

Figure 1 | Study location.

components:

$$SW_t = SW_0 + \sum_{i=1}^{t} (R_{day} - Q_{surf} - E_a - W_{seep} - Q_{gw}) \quad (1)$$

where SW_t is the soil water content at time t; SW_0 is initial soil water content; t is time (in days); R_{day} is the amount of precipitation per day; Q_{surf} is the amount of surface runoff on day; E_a is the amount of evapotranspiration per day; W_{seep} is the water percolation to the bottom of the soil profile per day; Q_{gw} is the amount of water returning to the groundwater per day.

Some of the inputs required for the SWAT run include land use data, soil data and slope information, precipitation and temperature data of the watershed. The model was calibrated from 2003 to 2010. At this stage, the model was fine tuned for various parameters governing the stream flow at the selected outlet of the watershed. The sensitivity analysis using SWAT Calibration Uncertainties Program (SWAT-CUP) with Sequential Uncertainty Fitting ver.2 (SUFI-2) was carried out to calibrate the SWAT model. Statistical indices including the Nash–Sutcliffe coefficient of efficiency (NSE), correlation coefficient (R^2), percent bias (PBIAS), and relative error (RE) were used for validating the model performance. The parameters so tuned for modeling streamflow (on a monthly scale) are given in Table 1. To check the robustness of the model, validation was performed for the same values of parameters as in model calibration but from the years 2011–2013. The evaluation metrics of the model in the calibration period were $R^2 = 0.71$, PBIAS = 0.20, RE = 0.15, and NSE = 0.65, and $R^2 = 0.67$, PBIAS = 0.23, RE = 0.18, and NSE = 0.58 during the validation period. Curve number (CN) was observed to be the most sensitive parameter affecting streamflow generation in the watershed.

One of the main advantages of the SWAT run in the present study is obtaining a time series of monthly streamflow data at any desired location. However, this does come with limitations, which any physically distributed model

Table 1 | Sensitive analysis and calibration results using SUIF-2, SWATCUP

				Global sensitivity	
Parameter	**Min value**	**Max value**	**Fitted value**	***t*-stat**	***P*-value**
r__CN2.mgt	–0.25	0.15	–0.24	4.47	0.00
v__ALPHA_BF.gw	0	1	0.2	–4.14	0.00
v__GW_DELAY.gw	0	500	21.14	–2.92	0.00
v__GWQMN.gw	0	500	315.83	–2.40	0.02
v__SURLAG.bsn	0.05	30	10.76	–1.88	0.06
v__ESCO.hru	0	1	0.53	–1.82	0.07
v__EPCO.hru	0	1	0.97	1.74	0.08
v__OV_N.hru	0.1	0.3	0.18	–1.62	0.11
v__SLSUBBSN.hru	–0.5	0.5	0.1	–1.37	0.17
v__DEP_IMP.hru	0	6,000	5,074.6	–1.31	0.19
v__GW_REVAP.gw	0.2	0.2	0.05	–1.22	0.22
v__REVAPMN.gw	1	100	30.35	–1.14	0.26
v__CH_COV1.rte	0	0.6	0.04	1.13	0.26
v__CH_K2.rte	1	50	13.7	1.00	0.32
v__CH_N2.rte	0.01	0.3	0.08	0.99	0.32
r__SOL_AWC().sol	0.3	1	0.5	0.77	0.44
v__SOL_K().sol	0.25	25	2.22	–0.63	0.53
v__CH_K1.sub	0.05	5	2.24	0.61	0.54
v__CH_N1.sub	1	65	12.99	–0.50	0.61
v__CH_S1.sub	–0.5	1	–0.18	–0.49	0.62
r__SOL_Z().sol	0	0.05	0.03	0.46	0.64
r__GDRAIN.mgt	–0.25	0.25	–0.18	–0.44	0.66
v__SFTMP.bsn	–5	5	–4.46	–0.44	0.66
r__HRU_SLP.hru	0	0.6	0.14	0.43	0.66
r__RCHRG_DP.gw	0	1	0.11	0.37	0.71
r__SOL_CBN().sol	0.5	1	0.57	0.37	0.71
r__SOL_ALB().sol	0	0.25	0.1	–0.36	0.72
v__SMTMP.bsn	–5	5	3.55	0.32	0.75
v__SMFMX.bsn	1.7	6.5	3.79	–0.32	0.75
v__SMFMN.bsn	1.7	6.5	3.2	–0.32	0.75
r__SOL_ZMX.sol	0	0.05	0.05	–0.30	0.76
r__DDRAIN.mgt	–0.1	1	0.16	0.27	0.78
r__TDRAIN.mgt	–0.25	0.25	–0.07	–0.27	0.78
v__SHALLST.gw	0	1,000	902.56	0.25	0.80
v__DEEPST.gw	0	6,000	923.84	–0.15	0.88
v__CANMX.hru	0	100	83.48	–0.10	0.92
v__EVRCH.bsn	0.5	1	0.68	–0.09	0.92
v__LAT_TTIME.hru	0	180	154.85	–0.06	0.95
v__USLE_K().sol	0	0.65	0.38	0.03	0.98

v_ represents existing parameter value and will be replaced by the given value, and r_ represents the existing parameter and is multiplied by (1+ given value).

will have, such as uncertainty in the results because of the uncertain parameters and mathematical simplification of an otherwise complicated process of streamflow generation. Considering the fact that streamflow is an important variable representing hydrological drought, therefore, a relationship between observed precipitation vs. observed streamflow, and observed rainfall vs. modeled streamflow was found, as shown in Figure 2. With an acceptable value of R^2 as obtained, it was assumed that the modeled streamflow is acceptable within the given uncertainties in the calibrated parameters.

Drought estimation

Taking monthly data of precipitation depth, streamflow, and soil moisture time series data between 1979 and 2014 as inputs, the drought indices SPI, SSFI, and SSMI were calculated. An SPI for each month was computed by estimating the key coefficient of gamma distribution (Lin *et al.* 2014; Winkler *et al.* 2017), given in Equation (2):

$$g(x_k) = \frac{1}{\beta^{\alpha}\Gamma(\alpha)} x_k^{\alpha-1} e^{-x_k/\beta} \text{ for } x_k > 0 \quad (2)$$

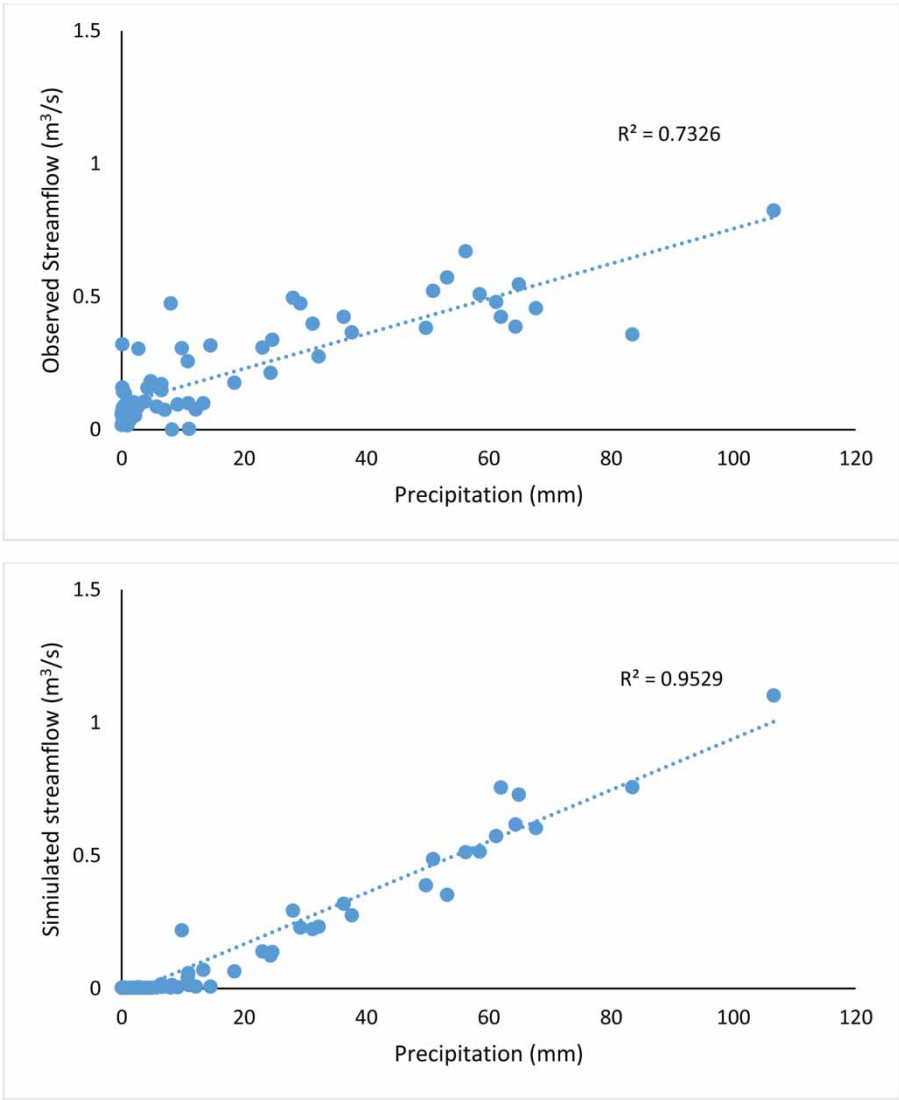

Figure 2 | Relationship between observed and simulated streamflow vs. precipitation.

Thereafter, the precipitation data was transformed to normally distributed SPI and described as (Lin *et al.* 2014; Winkler *et al.* 2017):

$$SPI = \frac{P - \overline{P}}{\sigma_P} \tag{3}$$

where P is the aggregated precipitation, as the respective mean, representing the standard deviation of available data (Keyantash 2016). Similarly, SSFI and SSMI were also computed based on the same procedure, but using streamflow and soil moisture as respective data inputs in estimation.

The magnitude of SPI, SSFI and SSMI is found to vary between –4 and +5. Figure 3 shows a time series plot of the three indices from January 1979 to December 2013. As seen in the figure, drought is found to have occurred almost every year during non-rainy months, and in the wet months (October–May). SPI and SSFI are observed to follow the same pattern. When SPI and SSFI are found to reduce, there is a considerable reduction in SSMI. This severity is found to coincide with the decreasing trend in SPI and SSFI during 1993–2001 (this is not visible in the figure) and 2003–2013.

Integrating the drought indices

Assignment of weights to the three variables is necessary for aggregating the effects of these variables in the proposed hybrid index. For these, two methods of weight assignment were used and compared. These methods are described below.

Entropy weight method

The entropy approach has been widely applied to measure the disorder degree of information in the field of information theory (Chang *et al.* 2016; Zhu *et al.* 2018). The method is adopted to reflect the difference of the index in different schemes. A high weight represents high differences with small entropies in the time series (Chang *et al.* 2016; Zhu *et al.* 2018). It takes an objective information measurement for weight estimation (Chang *et al.* 2016; Zhu *et al.* 2018). The entropy weight method (EW) is expressed as:

$$P_i = -k \sum_{j=1}^{n} f_{ij} \ln f_{ij},\ i = 1, 2, \ldots.., m \tag{4}$$

$$W_i = \frac{1 - P_i}{m - \sum_{i=1}^{m} P_i} \tag{5}$$

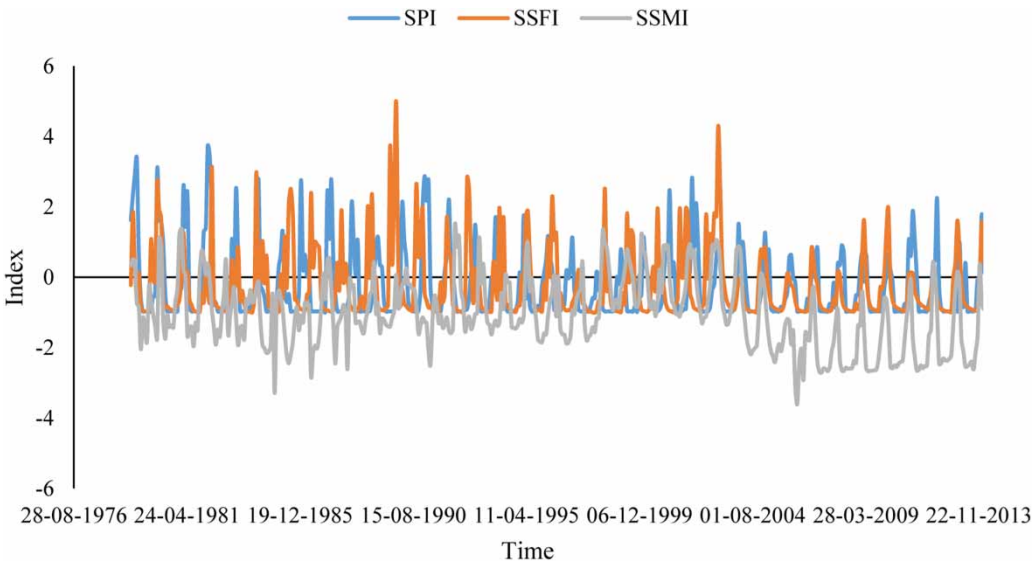

Figure 3 | Time series of SPI, SSFI, and SSMI for period January 1979–December 2013.

where f_{ij} is the frequency of the jth evaluating object in the ith index.

In order to better comprehend the data from both a seasonal and annual variation point of view, the entropy weights were found for one-, three-, six- and 12-month data for each variable under consideration.

Fuzzy-AHP method

The F-AHP method was also carried out to determine the weight for each drought index (SPI, SSFI, and SSMI). These indices were evaluated based on previous studies and expert opinion using a set of pairwise comparisons (PWC). Laarhoven & Pedrycz (1983) carried out the F-AHP method for the first time based on the logarithmic least squares method. The F-AHP has been involved in different fields due to its reasonable logic (Laarhoven & Pedrycz 1983). In this study, AHP was used to assign appropriate weights to an individual index (Saaty 1990). The general form of PWC matrix model, given by Saaty (2013), is as in Equation (6). In this study, the fuzzy number levels used to build the PWC matrix are given in Table 2:

$$A = a_{ij} = \begin{bmatrix} 1 & y_{12} & \cdots & y_{1n} \\ y_{21} & 1 & \cdots & y_{2n} \\ \vdots & \vdots & \vdots & \vdots \\ y_{m1} & y_{m2} & \cdots & 1 \end{bmatrix} = \begin{bmatrix} 1 & y_{12} & \cdots & y_{1n} \\ 1/y_{12} & 1 & \cdots & y_{2n} \\ \vdots & \vdots & \vdots & \vdots \\ 1/y_{1n} & 1/y_{21} & \cdots & 1 \end{bmatrix} \quad (6)$$

The element a_{ij} is a measure of the preference of the element of the row 'i' relative to the element of column 'j'. AHP assigns 1 to all elements of the diagonal of the pairwise comparison matrix. The weights matrix, $W = (w_1, w_2, \ldots w_n)$, were calculated based on the eigenvector method in Equation (7) (Saaty 1990) as:

$$\alpha_{ij} = \frac{a_{ij}}{\sum_{i=1}^{n} a_{ij}} \quad (7)$$

$$w_i = \frac{\sum_{i=1}^{n} \alpha_{ij}}{n} \quad (8)$$

The degree of coherence was applied to determine the consistency of importance of weight between the judgments in pairs provided by the decision-maker (where $CR < 0.1$ indicates consistent judgments):

$$\begin{bmatrix} 1 & y_{12} & \cdots & y_{1n} \\ y_{21} & 1 & \cdots & y_{2n} \\ \vdots & \vdots & \vdots & \vdots \\ y_{m1} & y_{m2} & \cdots & 1 \end{bmatrix} \times \begin{bmatrix} w_1 \\ w_2 \\ \vdots \\ w_n \end{bmatrix} = \begin{bmatrix} w'_1 \\ w'_2 \\ \vdots \\ w'_n \end{bmatrix} \quad (9)$$

$$\lambda_{\max} = \frac{1}{m} \times \left(\frac{w'_1}{w_1} + \frac{w'_2}{w_2} + \cdots + \frac{w'_n}{w_n} \right) \quad (10)$$

Following which the consistency index (CI) and the consistency ratio (CR) given by Equations (11) and (12) were calculated. In general, $CI < 0.1$ is taken as the tolerable error range (Saaty 1990):

$$CI = \frac{\lambda_{\max} - n}{n - 1} \quad (11)$$

$$CR = \frac{CI}{RI} \quad (12)$$

Table 3 provides all possible values of the random index, corresponding to the given number of variables.

The weights so obtained by the two methods given above are shown in Table 4. Based on the values obtained, it can be concluded that the entropy weight method and F-AHP method will assign almost similar weights to three variables used in the estimation of drought index. In order of preference, precipitation has more weightage in terms of its importance in describing the drought-like condition while soil moisture has comparatively lesser weightage. Based on the comparison between these methods, it can be clearly seen that the monthly SPI series has the largest

Table 2 | Fuzzy number levels as in the present study

Fuzzy number	Linguistic variable
1	Equally important
3	Moderately important
5	Strongly important
7	Very strongly important
9	Extremely important
2, 4, 6, 8	Intermediate values between adjacent scale values

Table 3 | Random index (RI)

N	1	2	3	4	5	6	7	8	9	10
RI	0.00	0.00	0.58	0.90	1.12	1.24	1.32	1.41	1.45	1.49

N refers to number of variables.

Table 4 | Weight assignment based on F-AHP and entropy method

Method	Precipitation	Streamflow	Soil moisture
F-AHP	0.3750	0.3333	0.2917
Entropy weight (monthly)	0.3619	0.3381	0.3000
Entropy weight (three-month)	0.3687	0.3248	0.3065
Entropy weight (six-month)	0.3559	0.3327	0.3114
Entropy weight (12-month)	0.3560	0.3295	0.3145

weight, whereas the monthly SSMI series has the smallest weight which also corroborates with the studies made by Chang *et al.* (2016) and Zhu *et al.* (2018).

Estimation of hybrid drought index (HDI)

Based on the analysis in the previous section, the three selected indices were divided into ten classes that ranged between extreme wet to extreme drought (Table 5). The EW, SW, MW, LW, AW, AD, LD, MD, SD, and ED denote extreme wet, severe wet, moderate wet, light wet, abnormal wet, abnormal drought, light drought, moderate drought, severe drought, and extreme drought, respectively.

The assumption of a hybrid drought index is to build an indicator matrix with c classes and m indices and is expressed as follows (Zhu *et al.* 2018):

$$Y = \begin{bmatrix} <a_{12} & [a_{12}, b_{12}] & \ldots.. & [a_{1(c-1)}, b_{1(c-1)}] & >b_{1(c-1)} \\ >a_{22} & [a_{22}, b_{22}] & \ldots.. & [a_{2(c-1)}, b_{2(c-1)}] & <b_{2(c-1)} \\ \vdots & \vdots & \vdots & \vdots & \vdots \\ <a_{m2} & [a_{m2}, b_{m2}] & \ldots.. & [a_{m(c-1)}, b_{m(c-1)}] & <b_{m(c-1)} \end{bmatrix} \tag{13}$$

To calculate this, Equation (14) was used to first transform the matrix Y:

$$= \begin{cases} y_{i1} = a_{i2} \\ y_{ih} = \dfrac{a_{ih} + b_{ih}}{2}, h = 2, 3, \ldots.., (c-1) \\ y_{ic} = {}_{bi(c-1)} \end{cases} \tag{14}$$

where a_{ih} and b_{ih} are the left and right boundary values of the hth index in the ith class, respectively:

$$Y = \begin{bmatrix} y_{11} & y_{12} & \ldots. & y_{1c} \\ y_{21} & y_{21} & \ldots. & y_{2c} \\ \vdots & \vdots & \vdots & \vdots \\ y_{m1} & y_{m2} & \ldots. & y_{mc} \end{bmatrix} = (y_{ih}) \tag{15}$$

Table 5 | HDI system of drought

Drought types	Drought indices	Drought classes									
		EW	SW	MW	LW	AW	AD	LD	MD	SD	ED
Metrological drought	SPI	>1.6	[1.3,1.6]	[0.8,1.3]	[0.5,0.8]	[0,0.5]	[–0.5,0]	[–0.8,–0.5]	[–1.3,–0.8]	[–1.3,–1.6]	<–1.6
Hydrological drought	SSFI	>1.6	[1.3,1.6]	[0.8,1.3]	[0.5,0.8]	[0,0.5]	[–0.5,0]	[–0.8,–0.5]	[–1.3,–0.8]	[–1.3,–1.6]	<–1.6
Agriculture drought	SSMI	>1.6	[1.3,1.6]	[0.8,1.3]	[0.5,0.8]	[0,0.5]	[–0.5,0]	[–0.8,–0.5]	[–1.3,–0.8]	[–1.3,–1.6]	<–1.6

The EW, SW, MW, LW, AW, AD, LD, MD, SD, and ED denote extreme wet, severe wet, moderate wet, light wet, abnormal wet, abnormal drought, light drought, moderate drought, severe drought, and extreme drought, respectively.

Suppose that x_i of the ith index lies in $[y_{ih}, y_{ih+1}]$, the relative membership of x_i to the hth class is calculated as:

$$\mu_{ih}(u) = \frac{y_{ih+1}^{-i(h+1)} x_i}{y_{ih+1}^{-i(h+1)} y_{ih}}, h = 1, 2, \ldots., c-1 \quad (16)$$

In addition, the relative membership degree to the rest of the classes is zero. Then, the indices matrix of the relative membership degree can be obtained. The relative membership degree of evaluating object to h class is computed as:

$$\upsilon_h(u) = \sum_{i=1}^{m} \omega_i * \mu_{\mathrm{ih}}(\mathrm{u}) \quad (17)$$

$$HDI = \sum_{i=1}^{m} \omega_i B_i \quad (18)$$

where x_i denotes the weight of the ith index, B_i is the weight of drought class, and $\sum_{i=1}^{m} \omega_i = 1$. The characteristic value of the evaluating object is calculated as follows:

$$H(u) = \sum_{i=1}^{c} \upsilon_h(u) \times h_i \quad (19)$$

where H represents the Hurst index.

Table 5 shows the HDI system of drought, defining the values of different drought indices falling in different drought classes.

Wavelet analysis for index validation

Wavelet analysis can be useful in studying the periodicity of the component, e.g. rainfall, streamflow, soil moisture, and drought indices. In drought analysis, it can be useful in analyzing drought patterns, drought trend and drought periodicity from a given index, along with the relationships between drought conditions and teleconnections (Thomas & Prasannakumar 2016; Wang *et al.* 2017; Guo *et al.* 2018). Li *et al.* (2020) have used continuous wavelet transform, cross wavelet transform, wavelet coherence and wavelet cross-correlation to determine the relationship and links between meteorological drought and hydrological drought.

For analyzing the association among two-time series, it was required that a bivariate structure called wavelet coherence was first described. In support of the appropriate description of wavelet coherence, it first requires the description of the cross wavelet transform and cross-wavelet power (Afshan *et al.* 2018; Zhu *et al.* 2018). The details of these techniques can be found in Afshan *et al.* (2018). According to Torrence & Compo (1998), cross wavelet transform can be explained by two-time sequences, $x(t)$ and $y(t)$, as:

$$W_{xy}(m, n) = W_x(m, n) W_y^*(m, n) \quad (20)$$

where $W_x(m, n)$ and $W_y(m, n)$ are two continuous wavelet transform of $x(t)$ and $y(t)$, separately, m is location index, and n represents the measure, whereas the sign * signifies a composite conjugate. The cross wavelet power could simply be calculated by the cross wavelet transform as $|W_x(m, n)|$. Furthermore, the cross wavelet power spectra disclose regions in the time sequence frequency space, where the time sequence displays a massive mutual power that it symbolizes in the confined covariance among the time sequence at every measure (Afshan *et al.* 2018). The wavelet coherence can identify areas in the time-frequency gap where the observed time series change simultaneously, but do not essentially have massive mutual power. According to Torrence & Webster (1999), the equation of adjusted wavelet coherence coefficient is as follows:

$$R^2(m, n) = \frac{|N(N^{-1} W_{xy}(m, n)|^2}{N(N^{-1}|W_x(m, n)|^2 N(N^{-1}|W_y(m, n)|^2} \quad (21)$$

Figure 4 displays the continuous wavelet transform between meteorological, hydrological, agricultural-based drought indices and the hybrid drought index. In the figure, the thick curved line represents the cone of influence (CoI); the dashed line is the significance level (5%) for the global wavelet spectrum. Based on Figure 4, it is found that the periodicity of drought predominately occurs within a one year band, meaning the drought had a frequency of occurrence once every year.

The wavelet coherence locates the sections in time-frequency in which the time series co-vary. Figures 5 and 6 provide interesting findings and the results clearly show the areas with a strong relationship between the datasets.

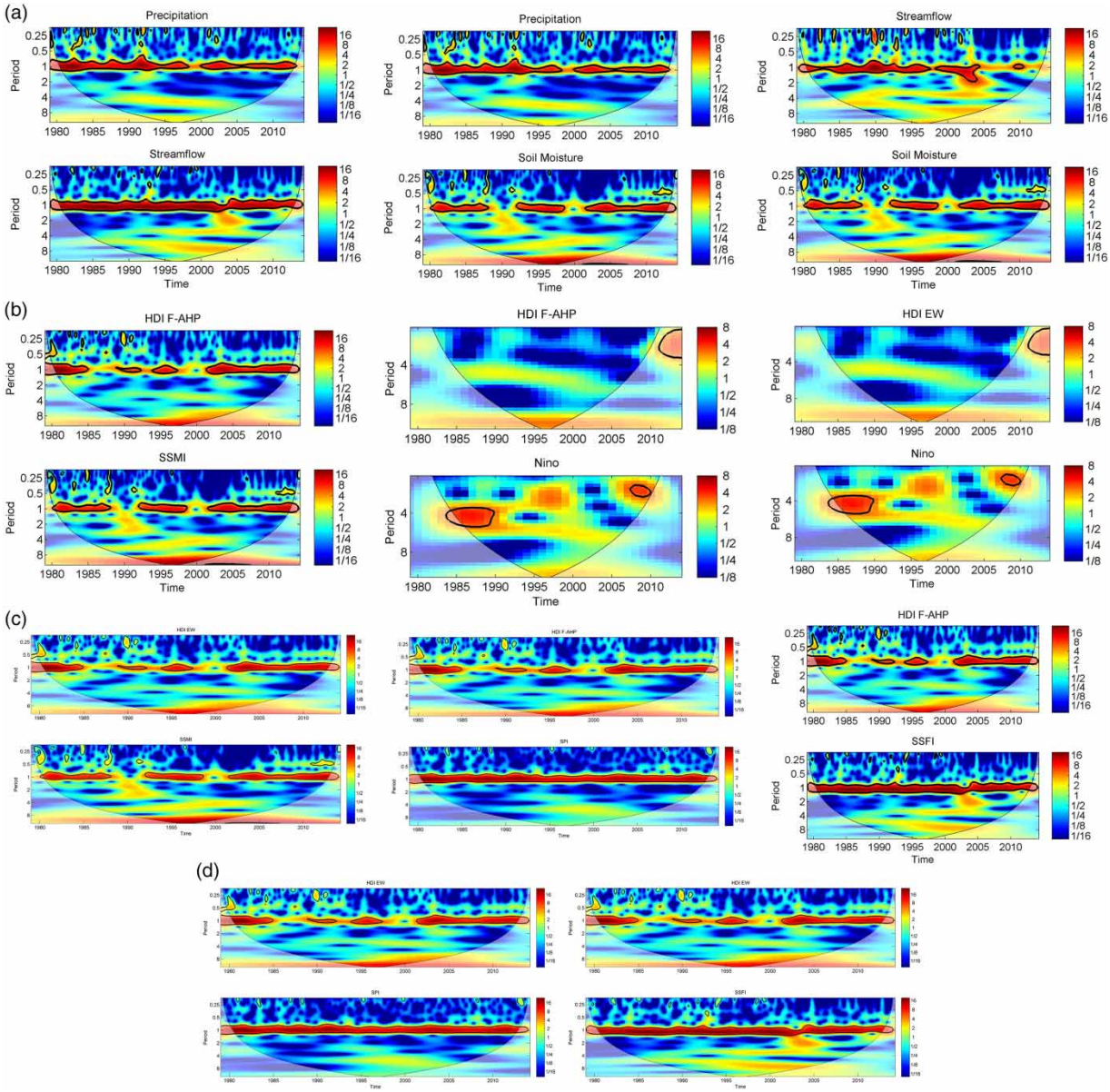

Figure 4 | Continuous wavelet power spectra for the time series of the transform relationships of: (a) rainfall, streamflow, and soil moisture, (b) HDI using F-AHP with SPI, SSFI, and SSMI, (c) HDI using ET weight with SPI, SSFI, and SSMI, (d) HDI using F-AHP with sunspot number Nino3.4 index.

In comparison between XWT and WTC results, high power coherence is observed in all regions of time series.

RESULTS AND DISCUSSION

After having worked out the drought indices, Pearson correlation coefficient (PCC) with 0-, 1-, 3-, and 6-lag was used to analyze the drought delay in the response parameter. The results obtained are given in Table 6. A high correlation coefficient between SPI and SSFI/SSMI indicates that precipitation is a significant parameter. In a one-month accumulation period, it can be observed from the table that the drought condition quickly changed between months as the PCC coefficient between SPI and SSMI are high ($r = 0.53$) and SPI and SSFI ($r = 0.38$), while the

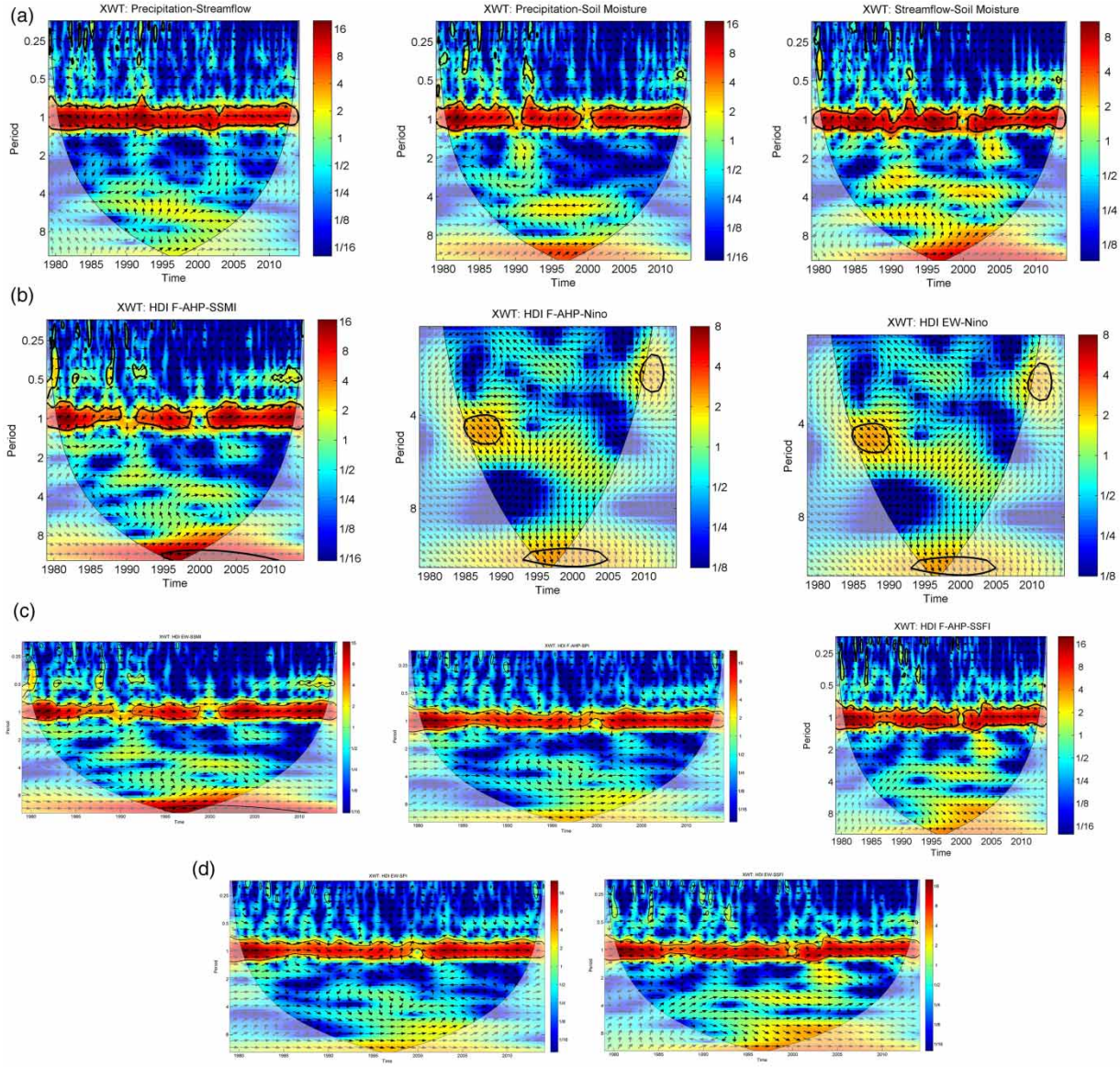

Figure 5 | The cross wavelet transform between: (a) rainfall, streamflow, and soil moisture, (b) HDI using F-AHP with SPI, SSFI, and SSMI, (c) HDI using ET weight with SPI, SSFI, and SSMI, (d) HDI using F-AHP with sunspot number Nino3.4 index.

response of soil moisture to streamflow is found to be weak ($r = 0.49$) at a different lag time. Also, the three-month accumulation period shows better performance in comparison to a shorter timescale for detecting the drought. The six- and 12-month periods showed similar results to other periods in the case of response of the soil moisture to precipitation, while on the other hand the response of soil moisture to streamflow was clearly shown by PCC values as it increased from $r = 0.55$ to $r = 0.63$. The long-term timescale analysis, i.e. 12-month accumulation period, shows that the drought is controlled by streamflow. Based on PCC analysis, it is found that monthly and three-month cumulative periods were useful in analyzing and detecting short-term behavior, while six- and 12-month periods were able to capture a long-term behavior and hence these periods are more suitable for studying the drought conditions in the area.

To further detect the sudden changes in the time series data of precipitation, streamflow, and soil moisture data, along with the drought indices computed above, a trend

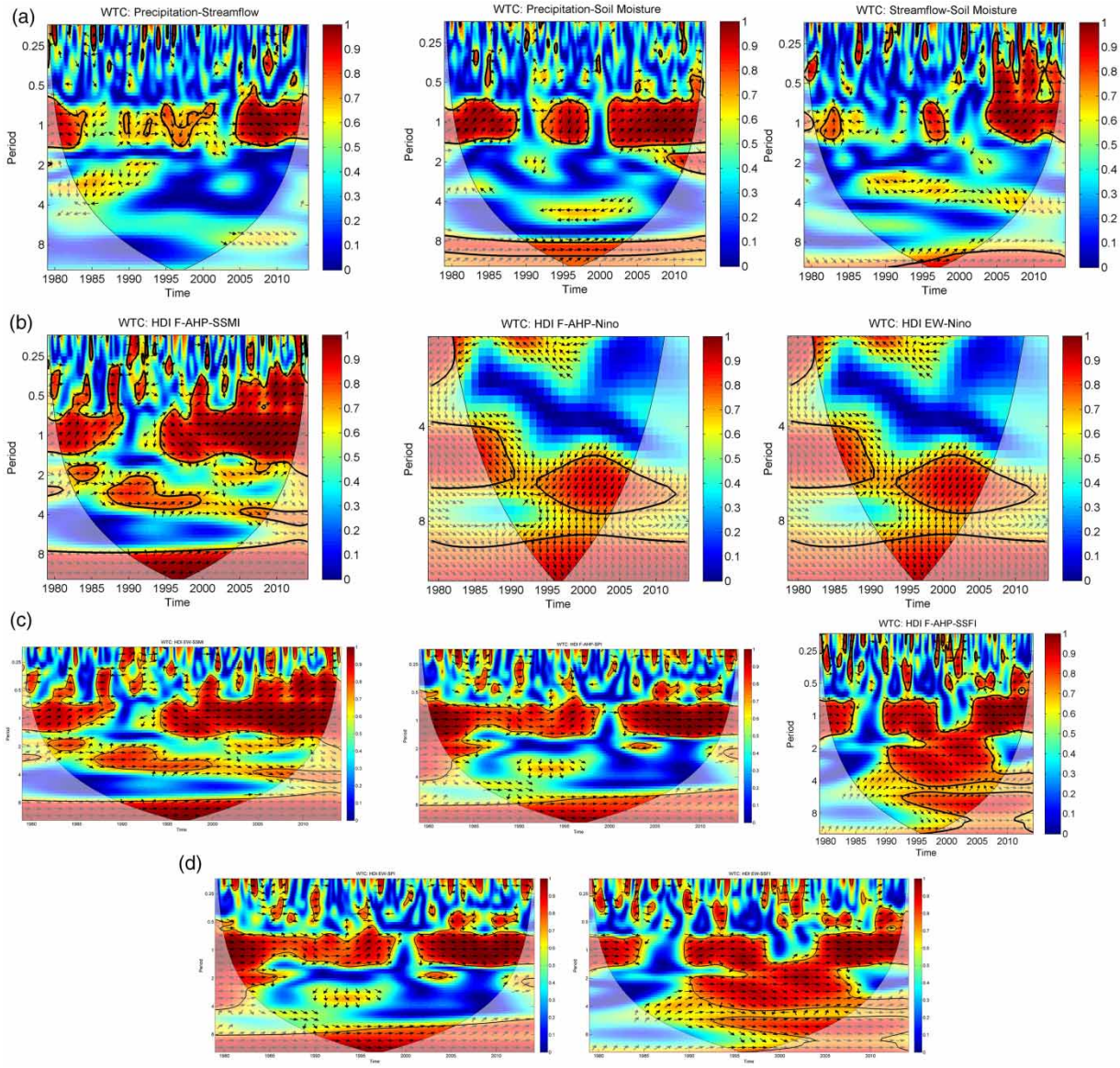

Figure 6 | Wavelet coherence (WCO) between: (a) rainfall, streamflow, and soil moisture, (b) HDI using F-AHP with SPI, SSFI, and SSMI, (c) HDI using ET weight with SPI, SSFI, and SSMI, (d) HDI using F-AHP with sunspot number Nino3.4 index.

analysis was performed using the innovative trend analysis method proposed by Şen (2012). Although various other methods are available to detect the trend in time series data, this method was chosen over other methods for two reasons; first, this method generates seven possible trend conditions compared to trendless, increasing trend and decreasing trend, and second, this method gave better validation when used to predict trends in precipitation data for the same area in a previous study (Al Balasmeh *et al.* 2019).

The analysis of this method on the dataset revealed a trend in both monthly and seasonal precipitation, streamflow, soil moisture, and their related indices. Table 7 shows that the ITA detected a trend in precipitation, streamflow, and soil moisture data based on monthly data. Low, medium, high trend, and trendless were detected for all datasets. In summer months, the trend shows similarity with rainy months for precipitation, streamflow, and soil moisture, owing to the fact that

Table 6 | PCC analysis for drought indices

Monthly data

Lag 0	SPI	SSFI	SSMI	Lag 3	SPI	SSFI	SSMI
SPI	1.00			SPI	1.00		
SSFI	0.38	1.00		SSFI	0.36	1.00	
SSMI	0.53	0.49	1.00	SSMI	0.51	0.49	1.00
Lag 1	**SPI**	**SSFI**	**SSMI**	**Lag 6**	**SPI**	**SSFI**	**SSMI**
SPI	1.00			SPI	1.00		
SSFI	0.38	1.00		SSFI	0.37	1.00	
SSMI	0.53	0.49	1.00	SSMI	0.51	0.49	1.00

3-month period

Lag 0	SPI-3	SSFI-3	SSMI-3	Lag 3	SPI-3	SSFI-3	SSMI-3
SPI-3	1.00			SPI-3	1.00		
SSFI-3	0.42	1.00		SSFI-3	0.40	1.00	
SSMI-3	0.57	0.54	1.00	SSMI-3	0.56	0.54	1.00
Lag 1	**SPI-3**	**SSFI-3**	**SSMI-3**	**Lag 6**	**SPI-3**	**SSFI-3**	**SSMI-3**
SPI-3	1.00			SPI-3	1.00		
SSFI-3	0.41	1.00		SSFI-3	0.40	1.00	
SSMI-3	0.56	0.54	1.00	SSMI-3	0.56	0.54	1.00

6-month period

Lag 0	SPI-6	SSFI-6	SSMI-6	Lag 3	SPI-6	SSFI-6	SSMI-6
SPI-6	1.00			SPI-6	1.00		
SSFI-6	0.40	1.00		SSFI-6	0.39	1.00	
SSMI-6	0.55	0.55	1.00	SSMI-6	0.54	0.55	1.00
Lag 1	**SPI-6**	**SSFI-6**	**SSMI-6**	**Lag 6**	**SPI-6**	**SSFI-6**	**SSMI-6**
SPI-6	1.00			SPI-6	1.00		
SSFI-6	0.39	1.00		SSFI-6	0.39	1.00	
SSMI-6	0.54	0.55	1.00	SSMI-6	0.54	0.55	1.00

12-month period

Lag 0	SPI-12	SSFI-12	SSMI-12	Lag 3	SPI-12	SSFI-12	SSMI-12
SPI-12	1.00			SPI-12	1.00		
SSFI-12	0.40	1.00		SSFI-12	0.40	1.00	
SSMI-12	0.48	0.63	1.00	SSMI-12	0.48	0.63	1.00
Lag 1	**SPI-12**	**SSFI-12**	**SSMI-12**	**Lag 6**	**SPI-12**	**SSFI-12**	**SSMI-12**
SPI-12	1.00			SPI-12	1.00		
SSFI-12	0.40	1.00		SSFI-12	0.40	1.00	
SSMI-12	0.48	0.63	1.00	SSMI-12	0.48	0.63	1.00

Table 7 | Trend identification for various parameters

	ITA		
Monthly	**L**	**M**	**H**
Streamflow	Y-	Y-	Y-
Streamflow_3-month	Y-	Y-	Y-
Streamflow_6-month	Y-	Y-	Y-
Streamflow_12-month	Y-	Y-	N
Soil moisture	Y-	Y-	Y-
Soil moisture_3-month	Y-	Y-	Y-
Soil moisture_6-month	Y-	N	Y-
Soil moisture_12-month	Y-	N	Y-
Precipitation	Y-	Y-	Y-
Precipitation_3-month	Y-	Y-	Y-
Precipitation_6-month	Y-	Y-	Y-
Precipitation_12-month	Y-	Y-	Y-
SSFI	Y-	Y-	Y-
SSFI-3	Y-	Y-	Y-
SSFI-6	Y-	Y-	Y-
SSFI-12	Y-	Y-	N
SSMI	Y-	N	Y-
SSMI-3	Y-	N	Y-
SSMI-6	Y-	Y-	Y-
SSMI-12	Y-	N	Y-
SPI	Y-	Y-	Y-
SPI-3	Y-	Y-	Y-
SPI-6	Y-	Y-	Y-
SPI-12	Y-	Y-	Y-
HDI	Y-	Y-	Y-
	ITA		
Seasons	**L**	**M**	**H**
Rainy_Streamflow	Y-	Y-	Y-
Rainy_Soil moisture	Y-	Y-	Y-
Rainy_Precipitation	Y-	Y-	Y-
Rainy_SSFI	Y-	Y-	Y-
Rainy_SSMI	Y-	N	Y-
Rainy_SPI	Y-	Y-	Y-
Rainy_HDI	Y-	Y-	Y-
Summer_Streamflow	Y-	Y-	Y-
Summer_Soil moisture	Y-	Y-	Y-
Summer_Precipitation	N	N	Y-
Summer_SSFI	Y-	Y-	Y-
Summer_SSMI	Y-	Y-	Y-
Summer_SPI	N	N	Y-
Summer_HDI	Y-	Y-	Y-

Y- refers to decrease trend and N refers to trendless.

precipitation is the principal form of water delivery. In essence, Wadi Shueib catchment experienced a dry trend on monthly and seasonal scales during the years 1979–2014.

The Hurst index was found to be more than 0.5. Different values of Hurst indices refer to types of time series. The three possible values for the Hurst index are: (i) $H < 0.5$, which refers to the trend of time series which, in the future, will be opposite to the current and past trend observed; (ii) $H = 0.5$ shows that the time series is independent; and (iii) $H > 0.5$ shows that the trend in the future will be similar to the current and past trends observed (Gammel 1998). Thus, the Hurst index can be applied to analyze the persistence of drought in the Wadi Shueib catchment. It can be easily observed from Figure 7 that the drought indices are following a trend, which is consistent with the finding of Törnros & Menzel (2014) and Rajsekhar & Gorelick (2017). For verifying the performance of HDI as a multi variables index against single drought indices, the times series plot of SPI, SSFI, and SSMI were compared with HDI, as shown in Figure 7(a). From the figure it can be observed that HDI follows a similar trend to other indices. For the sake of more clarity, the period between 2006 and 2008 has been highlighted in Figure 7(b). From Figure 7(b) the trend can be clearly seen between HDI and other drought indices, and the trend is seen to almost relate with respect to other drought indices, the increase and decrease of SPI, SSFI, and SSMI also reflect a similar HDI trend. This indicates that HDI can reflect even a small change in the single variable indices, thus allowing for comprehensive characterizations of meteorological, hydrological and agricultural droughts. Based on the PCC test, as given in Table 8, a strong correlation is evident between HDI and SPI, SSFI, and SSMI.

Thus on the basis of the preliminary analysis, reliability of the proposed HDI model is established, which was further established by performing trend analysis using the wavelet analysis approach given in the wavelet analysis for validation section above. Figures 5(b) and 5(c) and 6(b) and 6(c) display the wavelet analysis between hybrid drought indices (HDI) using F-AHP and entropy weight (EW) and standardized drought indices (SPI, SSFI, and SSMI). No significant variation was observed in the analysis. A significant positive correlation

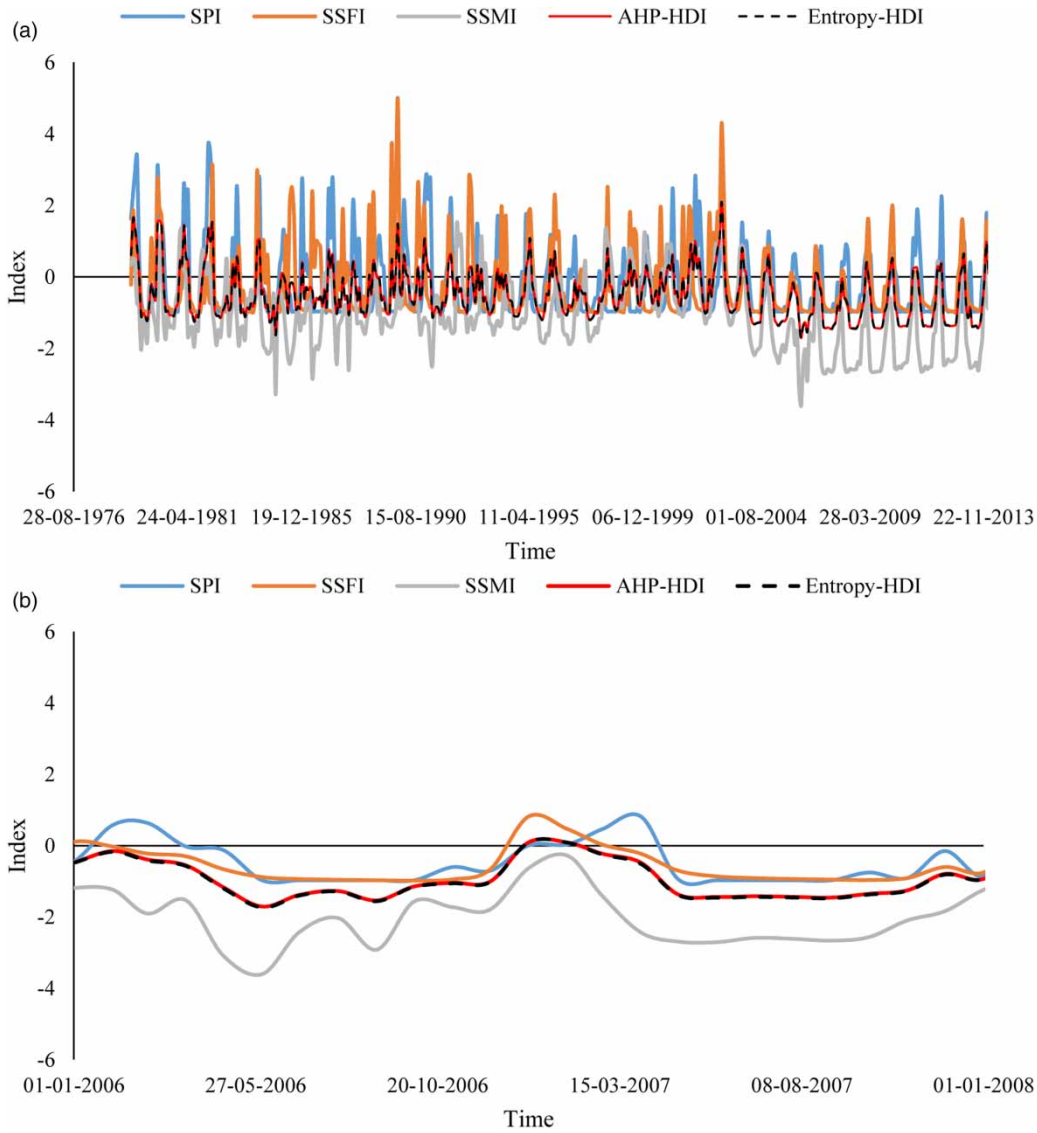

Figure 7 | Drought propagation for the basin during: (a) the period 1979–2014, (b) the period 2006–2007.

Table 8 | PCC analysis between HDI and other drought indices

Method	With SPI	With SSFI	With SSMI
F-AHP-HDI	0.91	0.84	0.73
Monthly Entropy-HDI	0.91	0.84	0.74
3-month Entropy-HDI	0.95	0.88	0.89
6-month Entropy-HDI	0.94	0.89	0.85
12-month Entropy-HDI	0.67	0.85	0.75

was found between HDI and other indices in the one-year signal, for all dataset series. The wavelet coherence supports this relationship since strong positive correlation clearly appears in the time series. Studying the relations between drought variations and climatic patterns such as Niño3.4 is helpful to understand the drought mechanism and evaluate the effect of atmospheric circulation on regional drought characteristics (Guo *et al.* 2018). Hence, large-scale sunspot activity (Niño3.4 index) was used to further conclude the validation of the proposed index (Zhu *et al.* 2018). Figures 5(d) and 6(d) represent the relations between the proposed index with the Niño index. It is found that HDI shows a statistically significant positive relationship with 1–3 years signal in 2008–2012,

4–5 years signal in 1985–1990, and 10–12 years signal in 1993–2005.

After ensuring that the HDI has good relationships with SPI, SSFI, and SSMI, the HDI was studied to analyze the drought condition in the area. To better identify the drought characteristics, the drought trend was determined on the basis of monthly and seasonal datasets. Table 7 shows the trend of the drought based on HDI, where in the monthly and rainy season the drought trend is showing a decreasing trend compared to the previous years. Also, during the summer season, there was a decreasing trend at all drought trend levels. Based on the overall situation in Wadi Shueib catchment, the drought detected using HDI implies that the drought situation has an aggravating trend in the area.

Moreover, the drought duration is increasing from year to year. Wadi Shueib catchment is likely to experience a gradual decline in the wet months. Rajsekhar & Gorelick (2017) confirmed similar findings. Based on climate change modeling, they confirmed that meteorological drought condition events will increase with drought severity ranging from 26 to 37%.

It can be observed from Figure 7 that the SPI is more sensitive to capture the drought onset. Or in other words, the meteorological drought or deficiency in precipitation is responsible for the onset of various drought types, while the streamflow drought is more capable of determining the realistic drought persistence. Thus, HDI, as an integrated index, can be useful for drawing insights on the drought types and their contribution to characterizing a drought-like situation.

CONCLUSIONS

The context of drought varies from region to region, based on user requirements and/or indicators of variables used, but in general defines a situation which is having a lack of water availability. The integration of multi-variables/indices is important to provide reliable and relevant drought indicators, which shows the overall characterization of drought in the region. In this study, a hybrid drought index (HDI) was modeled using the fuzzy set theory that combined meteorological, hydrological, and agricultural drought information for Wadi Shueib catchment in Jordan. The weights for aggregating the variables were objectively determined by using the F-AHP and entropy weight methods. The dataset that was used included precipitation, soil moisture, and streamflow data. While precipitation and soil moisture were readily available, streamflow was obtained after due calibration and validation of the SWAT model. Once the HDI was computed, several attempts were made to validate the index for the study area, which included trend analysis and cross wavelet analysis. Two methods, the entropy weight method and F-AHP were used for the assignment of weights which were then compared. On comparison, it was found that both the methods gave similar results, since the weights assigned by the two methods were found to be similar. Overall, the HDI showed its ability to address the drought condition in the area instead of using three different drought indices.

The study reveals a similarity in results produced by individual indices and HDI as both reveal a deficiency in the soil moisture, which is found to be increasing when compared to precipitation and streamflow from season to season. The HDI had captured the overall drought in the area and based on seasonal data (rainy and non-rainy months) the drought trend is found to increase. This conclusion corroborates with similar findings from the drought studies conducted in the Jordan Valley. Hence, it can be concluded that the proposed HDI in this study is a reliable indicator for drought characterization assessment, and it can be used to examine the drought characteristics in the area. Since the methodology used is generalized, it is envisaged that this study will be a potential tool for watershed managers and policymakers dealing with drought conditions in any geographical location.

REFERENCES

Afshan, S., Sharif, A., Loganathan, N. & Jammazi, R. 2018 Time–frequency causality between stock prices and exchange rates: further evidences from cointegration and wavelet analysis. *Phys. A Stat. Mech. Appl.* **495**, 225–244.

Al-Ansari, N. 2016 Hydropolitics of the Tigris and Euphrates Basins. *Engineering* **8**, 140–172.

Al Balasmeh, O., Babbar, R. & Karmaker, T. 2019 Trend analysis and ARIMA modeling for forecasting precipitation pattern in Wadi Shueib catchment area in Jordan. *Arabian J. Geosci.* **12**, 27.

Arnold, J. G., Srinivasan, R., Muttiah, R. S. & Williams, J. R. 1998 Large area hydrologic modeling and assessment: part I. Model development. *J. Am. Water Resour. Assoc.* **34**, 73–89.

Bazzaz, F. 1993 Global climatic changes and its consequences for water availability in the Arab world. In: *Water in the Arab Word: Perspectives and Prognoses* (R. Roger & P. Lydon, eds). Harvard University, Cambridge, MA, USA, pp. 243–252.

Chang, J., Li, Y., Wang, Y. & Yuan, M. 2016 Copula-based drought risk assessment combined with an integrated index in the Wei River Basin, China. *J. Hydrol.* **540**, 824–834.

Erhardt, T. M. & Czado, C. 2018 Standardized drought indices: a novel univariate and multivariate approach. *J. R. Stat. Soc. C Appl. Stat.* **67** (3), 643–664.

Favre, A. C., El Adlouni, S., Perreault, L., Thiémonge, N. & Bobée, B. 2004 Multivariate hydrological frequency analysis using copulas. *Water Resour. Res.* **40** (1), 1–12.

Gammel, B. M. 1998 Hurst's rescaled range statistical analysis for pseudorandom number generators used in physical simulations. *Phys. Rev. E* **58** (2), 2586–2597.

Gilbert, S. 2017 *Drought and Climate Change in Jordan: An Analysis of the 2008–2009 Drought and Climate Change Impact*. PhD Thesis, Pennsylvania State University, State College, PA, USA.

Griggs, D. J. & Noguer, M. 2002 Climate change 2001: the scientific basis. Contribution of working group I to the third assessment report of the intergovernmental panel on climate change. *Weather* **57** (8), 267–269.

Guo, H., Bao, A., Liu, T., Jiapaer, G., Ndayisaba, F., Jiang, L., Kurban, A. & De, M. P. 2018 Spatial and temporal characteristics of droughts in Central Asia during 1966–2015. *Sci. Total Environ.* **624**, 1523–1538.

Hao, Z. & AghaKouchak, A. 2013 Multivariate standardized drought index: a parametric multi-index model. *Adv. Water Resour.* **57**, 12–18.

Hayes, M. J., Wilhelmi, O. V. & Knutson, C. L. 2004 Reducing drought risk: bridging theory and practice. *Nat. Hazard. Rev.* **5** (2), 106–113.

Heim Jr., R. R. 2002 A review of twentieth-century drought indices used in the United States. *Bull. Am. Meteorol. Soc.* **83** (8), 1149–1165.

Huang, S. Z., Huang, Q., Chang, J. X., Zhu, Y. L., Leng, G. Y. & Xing, L. 2015 Drought structure based on a nonparametric multivariate standardized drought index across the Yellow River basin, China. *J. Hydrol.* **530**, 127–136.

Ionita, M., Dima, M., Lohmann, G., Scholz, P. & Rimbu, N. 2015 Predicting the June 2013 European flooding based on precipitation, soil moisture, and sea level pressure. *J. Hydrometeorol.* **16** (2), 598–614.

Jongman, B., Hochrainer-Stigler, S., Feyen, L., Aerts, J. C. J. H., Mechler, R., Botzen, W. J. W., Bouwer, L. M., Pflug, G., Rojas, R. & Ward, P. J. 2014 Increasing stress on disaster-risk finance due to large floods. *Nat. Clim. Change* **4** (4), 264–268.

Kao, S. C. & Govindaraju, R. S. 2010 A copula-based joint deficit index for droughts. *J. Hydrol.* **380** (1–2), 121–134.

Keyantash, J. 2016 *National Center for Atmospheric Research Staff. The Climate Data Guide: Standardized Precipitation Index (SPI)*. Available from: https://climatedataguide.ucar.edu/climate-data/standardized-precipitation-index-spi (accessed 22 January 2020).

Kwon, M., Kwon, H. H. & Han, D. 2019 Spatio-temporal drought patterns of multiple drought indices based on precipitation and soil moisture: a case study in South Korea. *Int. J. Climatol.* **39**, 4669–4687.

Laarhoven, M. V. & Pedrycz, W. 1983 A fuzzy extension of Saaty's priority theory. *Fuzzy Sets Syst.* **11** (1–3), 229–241.

Li, Q., He, P., He, Y., Han, X., Zeng, T., Lu, G. & Wang, H. 2020 Investigation to the relation between meteorological drought and hydrological drought in the upper Shaying River Basin using wavelet analysis. *Atmos. Res.* doi:10.1016/j.atmosres.2019.104743.

Lin, Z., Aifeng, L., Jianjum, W., Hayes, M., Zhenghong, T., Bin, T., Jiaghui, L. & Ming, L. 2014 Impact of meteorological drought on streamflow drought in Jinghe river basin of China. *Chin. Geogr. Sci.* **24** (6), 694–705.

McKee, T. B., Doesken, N. J. & Kleist, J. 1993 The relationship of drought frequency and duration to time scales. In: Proceedings of the 8th Conference on Applied Climatology, Boston, MA. *Am. Meteorol. Soc.* **17**(22), 179–183.

Mishra, A. K. & Singh, V. P. 2010 A review of drought concepts. *J. Hydrol.* **391** (1), 202–216.

Mohammad, A. H., Jung, H. C., Odeh, T., Bhuiyan, C. & Hussein, H. 2018 Understanding the impact of droughts in the Yarmouk Basin, Jordan: monitoring droughts through meteorological and hydrological drought indices. *Arab. J. Geosci.* **11**, 103.

Nury, A. H. & Hasan, K. 2016 Analysis of drought in Northwestern Bangladesh using standardized precipitation index and its relation to southern oscillation index. *Environ. Eng. Res.* **21** (1), 58–68.

Oertel, M., Meza, F. J., Gironás, J., Scott, C. A., Rojas, F. & Pineda-Pablos, N. 2018 Drought propagation in semi-arid river basins in Latin America: lessons from Mexico to the southern Cone. *Water* **10**, 1564.

Rajsekhar, D. & Gorelick, S. M. 2017 Increasing drought in Jordan: climate change and cascading Syrian land-use impacts on reducing transboundary flow. *Sci. Adv.* **3** (8), e170058. doi:10.1126/sciadv.1700581.

Rajsekhar, D. P., Singh, V. K. & Mishra, A. 2015 Multivariate drought index: an information theory based approach for integrated drought assessment. *J. Hydrol.* **526**, 164–182.

Real-Rangel, R. A., Pedrozo-Acuña, A. & Breña, J. A. 2020 A drought monitoring framework for data-scarce regions. *J. Hydroinform.* **22** (1), 170–185.

Roodposhti, S. M., Aryal, J., Shahabi, H. & Safarrad, T. 2016 Fuzzy Shannon entropy: a hybrid GIS-based landslide susceptibility mapping method. *Entropy* **18**, 343.

Saaty, T. L. 1990 How to make a decision: the analytic hierarchy process. *Eur. J. Oper. Res.* **48** (1), 9–26.

Saaty, T. L. 2013 The analytic network process. In *Decision Making with the Analytic Network Process*. International

Series in Operations Research & Management Science, Vol 95. Springer, Boston, MA.

Scherrer, S. C., Croci-Maspoli, M., Schwierz, C. & Appenzeller, C. 2006 Two-dimensional indices of atmospheric blocking and their statistical relationship with winter climate patterns in the Euro-Atlantic region. *Int. J. Climatol.* **26**, 233–249.

Şen, Z. 2012 Innovative trend analysis methodology. *J. Hydrol. Eng.* **17** (9), 1042–1046.

Shakhatreh, Y. 2010 Trend analysis for rainfall and temperatures in three locations in Jordan. In: *Food Security and Climate Change Conference, Proceedings International Center for Agricultural Research in the dry Areas (ICARDA)*, 1–4 February 2010, Amman, Jordan.

Sillmann, J. & Croci-Maspoli, M. 2009 Present and future atmospheric blocking and its impact on European mean and extreme climate. *Geophys. Res. Lett.* **36**, L1072.

Tarawneh, Z. S. 2011 Water supply in Jordan under drought conditions. *Water Pol.* **13**, 863–876.

Thomas, J. & Prasannakumar, V. 2016 Temporal analysis of rainfall (1871–2012) and drought characteristics over a tropical monsoon-dominated State (Kerala) of India. *J. Hydrol.* **534**, 266–280.

Törnros, T. & Menzel, L. 2014 Addressing drought conditions under current and future climates in the Jordan River region. *Hydrol. Earth Syst. Sci.* **18**, 305–318.

Torrence, C. & Compo, G. P. 1998 A practical guide to wavelet analysis. *Bull. Am. Meteorol. Soc.* **79** (1), 61–78.

Torrence, C. & Webster, P. 1999 Interdecadal changes in the ENSO–Monsoon System. *J. Climate.* **12** (8), 2679–2690.

Wang, Z., Li, J., Lai, C., Zeng, Z., Zhong, R., Chen, X., Zhou, X. & Wang, M. 2017 Does drought in China show a significant decreasing trend from 1961 to 2009? *Sci. Total Environ.* **579**, 314–324.

Wilhite, D. A. & Glantz, M. H. 1985 Understanding the drought phenomenon: the role of definitions. *Water Int.* **10**, 111–120.

Winkler, K., Gessner, U. & Hochschild, V. 2017 Identifying droughts affecting agriculture in Africa based on remote sensing time series between 2000–2016: rainfall anomalies and vegetation condition in the context of ENSO. *Remote Sens.* **9** (8), 831.

Yang, X., Zhang, L., Wang, Y., Singh, V. P., Xu, C., Ren, L., Zhang, M., Yi, L., Jiang, S. & Yuan, F. 2020 Spatial and temporal characterization of drought events in China using the severity-area-duration method. *Water* **12**, 230.

Zhang, L. & Singh, V. P. 2006 Bivariate flood frequency analysis using the copula method. *J. Hydrol. Eng.* **11** (2), 150–164.

Zhao, H., Yao, L., Mei, G., Liu, T. & Ning, Y. 2017 A fuzzy comprehensive evaluation method based on AHP and entropy for a landslide susceptibility map. *Entropy* **19**, 396.

Zhu, J., Zhou, L. & Huang, S. 2018 A hybrid drought index combining meteorological, hydrological, and agricultural information based on the entropy weight theory. *Arab. J. Geosci.* **11**, 91.

Zseleczky, L. & Yosef, S. 2014 *Are Shocks Really Increasing? A Selective Review of the Global Frequency, Severity, Scope, and Impact of Five Types of Shocks*. International Food Policy Research Institute, Addis Ababa, Ethiopia.

First received 19 February 2020; accepted in revised form 6 May 2020. Available online 12 June 2020